AIAA 93-0663

Shock Turbulence Interaction in the Presence of Mean Shear: an Application of Rapid Distortion Theory

K. Mahesh, S.K. Lele and P. Moin
Stanford University
Stanford, CA 94305

31st Aerospace Sciences Meeting & Exhibit
January 11-14, 1993 / Reno, NV

SHOCK TURBULENCE INTERACTION IN THE PRESENCE OF MEAN SHEAR: AN APPLICATION OF RAPID DISTORTION THEORY

Krishnan Mahesh, Sanjiva K. Lele* and Parviz Moin**
Department of Mechanical Engineering
Stanford University
Stanford, CA 94305

Abstract

Incompressible, homogeneous rapid distortion theory is used to examine the response of anisotropic turbulent flows to a shock wave. The shock wave is idealized as a one-dimensional compression and its effect on two canonical flows - shear flow and axisymmetric flow is studied. In the shear flow problem, both normal and oblique (with respect to the shear) compressions are considered.

Initial anisotropy defined in terms of $\overline{u_1^2}/q^2$ (x_1 is the shock-normal direction) affects the amplification of q^2, with higher initial $\overline{u_1^2}/q^2$ producing higher amplification. In the shear flow problem, normal compression amplifies all components of turbulent kinetic energy, with the shock-normal component being amplified the most. The amplification of q^2 for a fixed total volumetric strain (ρ/ρ_o) increases upon increasing the initial total shear (total shear is defined as the product of shear rate and the time of application of shear). Normal compression decreases the magnitude of $\overline{u_1u_2}/q^2$ and for large total volumetric strains, even changes its sign. Increasing the initial total shear hastens this trend. Examination of the terms in the $\overline{u_1u_2}$ evolution equation shows that the pressure-strain correlation is responsible for this behavior.

The oblique angle between the directions of compression and shear is seen to considerably affect the turbulence evolution. For a given total volumetric strain, the amplification of $\overline{u_1^2}$ decreases with increasing oblique angle (both positive and negative), while the amplification of $\overline{u_2^2}$ and $\overline{u_3^2}$ increases with oblique angle, for positive angles and decreases for negative angles (the shear is in the x_2 direction). Obliquity reduces the tendency of the magnitude of $\overline{u_1u_2}/q^2$ to decrease upon compression; for large oblique angles $\overline{u_1u_2}/q^2$ amplifies. Comparison of RDT to a compression-corner experiment shows good agreement in the evolution of $\overline{u_1u_2}/\overline{u_1^2}$, while the amplification of $\overline{u_1^2}$ is below the experimental value.

The effect of initial $\overline{u_1^2}/q^2$ on the amplification of q^2 is verified in the axisymmetric flow problem, where the amplification of q^2 for contracted turbulence is seen to be lower than that of isotropic turbulence which in turn is lower than the amplification of expanded turbulence.

1. Introduction

The modification of a turbulent flow due to its interaction with a shock wave is of importance in supersonic flows of engineering interest. In the vicinity of the shock, the mean flow dilatation is significant when compared to the mean flow vorticity, causing large changes in both the mean flow and turbulence across the shock wave. Turbulence closure models developed for low-speed shear flows were found unsuccessful in predicting the rapid changes in the region around the shock.[1] This lack of success is attributed to a lack of information on the behavior of the turbulence during the interaction and has prompted several experimental studies. Experimental work on shock wave/turbulence interaction has focussed mainly on the interaction between shock waves and turbulent boundary layers [2-10], with a few experiments studying shock wave/ free shear layer interaction.[11,12] The experiments find that turbulence intensities and Reynolds shear stress are amplified in the interaction. The shock structure is unsteady, leading to a region on the wall where the pressure signal is intermittent.

The flow field in the region of interaction is quite complex due to the simultaneous presence of mean shear, wall-blocking, streamline curvature and possible flow separation, in addition to direct influence of the shock wave. In order to isolate the effect of the shock, recent experiments have studied the interaction of shock waves with free turbulence such as grid turbulence[13,14] and turbulent jets.[12]

The numerical simulation of shock/turbulence interaction has thus far, been limited to isotropic turbulence interacting with a normal shock. Two-dimensional interaction was studied by Lee *et al.*[15] who solved the Navier Stokes equations and, Rotman[16] who solved the

* Also with Department of Aeronautics and Astronautics, Stanford University

** Also with NASA Ames Research Center

Euler equations. Recently, the interaction between three dimensional isotropic turbulence and a normal shock was numerically investigated by Lee *et al.*[17] who report a rise of turbulent kinetic energy in a region downstream of the intermittent zone occupied by the shock.

The theoretical analysis of shock/turbulence interaction is based on linearization of the turbulence into vorticity, acoustic and entropy modes and describing the interaction of each of these modes with the shock. This analysis (henceforth called LIA) was first developed by Ribner[18] and Moore[19] and subsequently by others such as Chang[20], Kerrebrock[21] and McKenzie and Westphal[22]. Ribner and Moore's analysis has been shown to agree well with experiments on shock/vortex interaction performed by Sekundov[23] and Dosanjh and Weekes[24] and, Rotman's two-dimensional computations of isotropic turbulence/normal shock interaction. Lee *et al*[15] use RDT to predict the response of isotropic turbulence to homogeneous one-dimensional compression. Idealizing the shock as a one-dimensional compression, they compare the RDT prediction of kinetic energy evolution to Ribner's LIA. The two analyses were seen to agree within 10% in predicting the amplification of the transverse velocity components for shock waves up to a Mach Number of 2.0 while, prediction of the amplification of the longitudinal velocity component agreed up to a Mach Number of 1.3.

Based on LIA and experimental data, Zang *et al* [25] suggested that there were at least four identifiable mechanisms responsible for the enhancement of turbulence across a shock wave. The primary mechanisms suggested were the amplification of incident vorticity and the conversion of incident acoustic and entropy waves into vorticity across the shock, while the focusing of vorticity by shock distortions and, conversion of mean flow energy into turbulence due to shock oscillations were listed as secondary mechanisms. The linear analyses mentioned above account for the primary mechanisms of turbulence amplification. While LIA seems closer to the physics of the problem than RDT, the agreement between the two for weak shocks suggests that in the weak-shock regime, RDT is a valid tool for analysis. As will be seen later, in experiments on shock wave/boundary layer interaction, the shock-normal Mach number is in the range of good agreement between LIA and RDT.

In this paper, we use RDT to study the response of homogeneous anisotropic turbulent flows to a shock wave. We idealize the shock as a one-dimensional compression and study its effect on turbulence that is constrained to be homogeneous. We consider two problems - sheared turbulence subjected to a one-dimensional compression, and axisymmetric turbulence compressed along the axis of axisymmetry. RDT is used to analyze the interaction. Section 2 outlines details of the theoretical procedure, and Sections 3 and 4 describe the results obtained.

2. Rapid Distortion Theory

RDT combines linearization of the governing equations with statistical averaging, to describe the statistical evolution of turbulence in the presence of rapid mean deformation. When the time scale of the mean deformation is much smaller than the characteristic time scale of the turbulence, the turbulence has no time to interact with itself. Generally, the flow is also constrained to be inviscid. These assumptions allow the neglect of all terms in the governing equations that involve viscosity or products of fluctuations, yielding the following set of equations that are linear in the fluctuations,

$$\frac{\partial u_i}{\partial x_i} = 0 \tag{1}$$

$$\frac{\partial u_i}{\partial t} + U_j \frac{\partial u_i}{\partial x_j} + u_j \frac{\partial U_i}{\partial x_j} = -\frac{1}{\rho}\frac{\partial p}{\partial x_i} \tag{2}$$

where, U_i and ρ are the mean velocity and density respectively, and u_i and p are the fluctuating velocity field and pressure respectively. The above set of equations corresponds to solenoidal turbulence and requires that the mean density be spatially uniform.

Since the turbulence is homogeneous, the mean velocity gradient is constrained to be spatially uniform; *i.e.*, the mean velocity is of the form $U_i = A_{ik}(t)x_k$. The spatial dependency of the mean velocity hampers solution of the above equations using Fourier transforms in $\mathbf{x}$. The spatial dependency may be removed however, by transforming the coordinate system to one that deforms with the mean field [26]; *i.e.*,

$$\xi_i = B_{ik}(t)x_k \qquad \tau = t$$

where,

$$\frac{d}{dt}B_{nk} + A_{jk}B_{nj} = 0 \tag{3}$$

The transformed equations are then Fourier transformed and solved. An alternative method of solution is to use Fourier representation in the original coordinates where the wavenumber changes with time as,

$$u(\mathbf{x},t) = \sum_{\mathbf{k}} \hat{u}(\mathbf{k},t)e^{ik_j(t)x_j}$$

where,

$$\frac{dk_\alpha}{dt} + k_j A_{j\alpha} = 0 \tag{4}$$

In this paper, except where indicated, the first method of solution was used.

One-dimensional strain is characterized by the following mean flow,

$$U_1 = \frac{\Gamma_o}{1+\Gamma_o t} x_1, \quad U_2 = U_3 = 0 \tag{5}$$

$$\rho = \frac{\rho_o}{1+\Gamma_o t} \tag{6}$$

$$P = \frac{P_o}{[1+\Gamma_o t]^\gamma} \tag{7}$$

where U_1, U_2, U_3 are the mean velocity components in the x_1, x_2, x_3 directions respectively; ρ and P are the mean density and pressure, respectively, and are uniform in space. Γ_o is negative for a compression and positive for an expansion. The mean field is thus, constrained by the *compressible* Euler equations and the requirement that the turbulence be homogeneous. As a consequence, the mean strain rate ($U_{1,1}$) varies with time. Note that the mean field being dilatational, the governing equations for the fluctuations (equations (1) and (2)) are obtained by linearization of the compressible Euler equations and correspond to the solenoidal component of the compressible flow field. The solenoidal component is assumed to be decoupled from the dilatational component; an assumption that is valid for the above mean flow if $\Delta m = \Gamma_o L/a \ll 1$ where, L is a lengthscale of the turbulence and a is the mean speed of sound [27]; *i.e.*, the turbulence is nearly incompressible. Since, under solenoidal RDT, the turbulence evolution is determined by the *total volumetric strain* (ρ/ρ_o) and not the strain rate, it would seem unnecessary that the mean field satisfy homogeneity for compressible fluctuations. However, the above form of the equations allows the contribution of the solenoidal component to compressible quantities like the pressure-dilatation correlation to be extracted from the analysis.

The evolution of the turbulence is determined entirely by its initial conditions and the total volumetric strain. Earlier studies[28,29] assume isotropic initial conditions; however, since our interest is in anisotropic turbulence interacting with shock waves, we consider anisotropic initial states. The importance of initial anisotropy in shock/turbulence interaction was noted by Jacquin *et al* [12] who showed within the framework of RDT that the evolution of the shock-normal component of turbulent kinetic energy upon compression is strongly dependent upon the initial energy spectrum. In their experiments on the interaction of isotropic turbulence and a turbulent jet with shock waves, the amplification of the streamwise component of turbulent

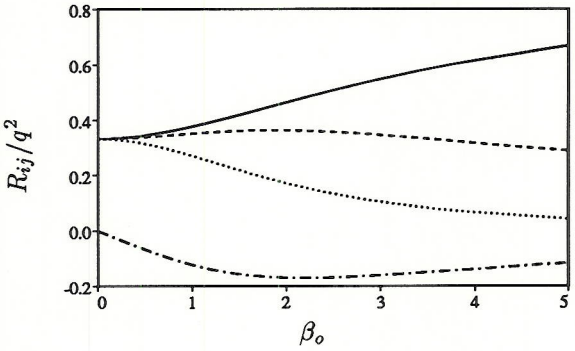

FIGURE 1. RDT prediction of the evolution of R_{ij}/q^2 with total shear: —— (R_{11}/q^2), ····· (R_{22}/q^2), ---- (R_{33}/q^2), —·— (R_{12}/q^2)

kinetic energy in the jet was higher than that for isotropic turbulence - a result they suggest, of either the anisotropy in the jet or extra production terms introduced by compressibility.

In this paper, two kinds of anisotropic turbulence are considered; sheared turbulence and axisymmetric turbulence. These states are obtained by RDT applied to initially isotropic turbulence that is subjected to shear in one case and axisymmetric strain in the other. The conditions prevailing at the start of compression are discussed in more detail in the sections that follow.

3. One-dimensional compression of sheared turbulence

3.1 Normal compression

In this section, we consider the one-dimensional compression of sheared turbulence. Isotropic turbulence is subjected to homogeneous mean shear *i.e.*,

$$U_1 = S_o x_2, \quad \rho = \rho_o, \quad P = P_o \tag{8}$$

where U_1 is the mean velocity in the x_1 direction, and ρ and P are the mean density and pressure respectively, which are uniform.

The shear is imposed till a non-dimensional time $\beta_o = S_o t_o$ at which point, one-dimensional compression is added; *i.e.*, for $t > t_o$,

$$U_1 = \frac{\Gamma_o}{1+\Gamma_o(t-t_o)} x_1 + \frac{S_o}{1+\Gamma_o(t-t_o)} x_2 \tag{9}$$

$$\rho = \frac{\rho_o}{1+\Gamma_o(t-t_o)} \tag{10}$$

$$P = \frac{P_o}{[1+\Gamma_o(t-t_o)]^\gamma} \tag{11}$$

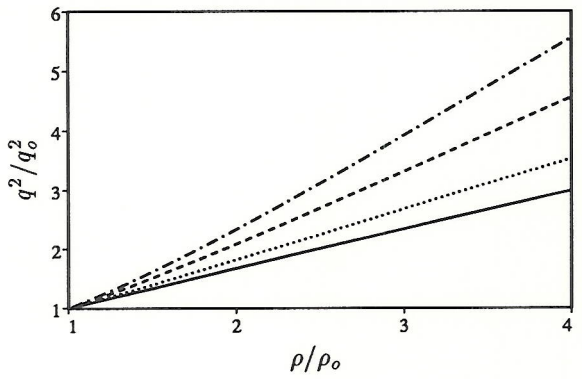

FIGURE 2. Evolution of kinetic energy for varying values of initial shear: —— (Isotropic), ····· ($\beta_o = 1$), ---- ($\beta_o = 2$), —·— ($\beta_o = 3$)

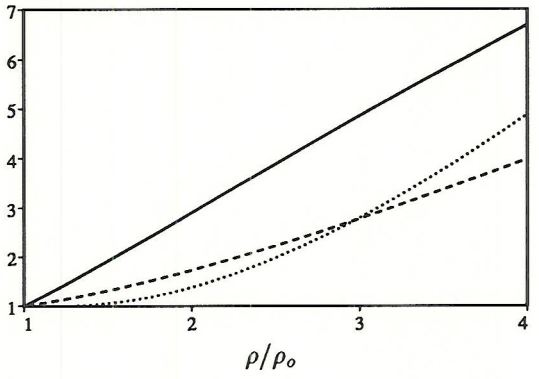

FIGURE 3. Amplification of the components of turbulent intensity ($\beta_o = 3$): —— ($\overline{u_1^2}$), ····· ($\overline{u_2^2}$), ---- ($\overline{u_3^2}$)

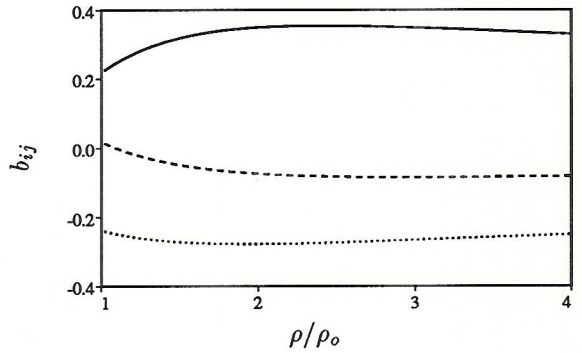

FIGURE 4. Evolution of Reynolds stress anisotropy ($\beta_o = 3$): —— (b_{11}), ····· (b_{22}), ---- (b_{33})

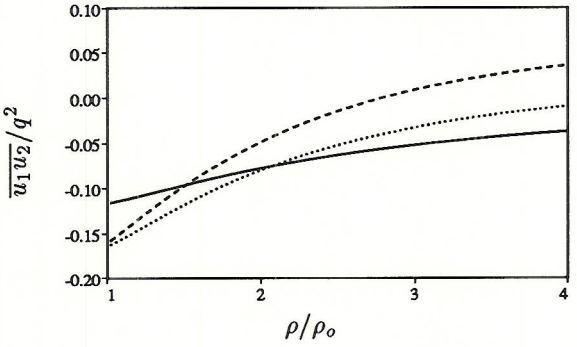

FIGURE 5. Evolution of $\overline{u_1u_2}/q^2$ for varying values of initial shear: —— ($\beta_o = 1$), ····· ($\beta_o = 2$), ---- ($\beta_o = 3$)

Variation of the shear rate with time during compression is necessary for the mean field to satisfy the compressible Euler equations. Note that the compression is along the x_1 axis while the shear is along x_2; we term this normal compression.

The state of the turbulence before compression depends only upon the total initial shear, β_o; its subsequent evolution depends upon β_o, the rate of shear compared to the rate of compression and the total volumetric strain. Since our interest is in shock/turbulence interaction, we consider the regime where the shear sets up the initial anisotropy and is negligible as compared to the subsequently applied compression; *i.e.*, $S_o/\Gamma_o \ll 1$. In this paper, S_o/Γ_o is 0.1 for all cases presented. Lower values of S_o/Γ_o (for *eg*, $S_o/\Gamma_o = 0.01$) yielded results identical to those shown here. Sheared turbulence is thus the initial state for the one-dimensional compression.

The effect of rapid homogeneous shear on initially isotropic turbulence has been studied using RDT by several authors.[30–33] Fig. 1 shows the evolution with total shear, of the Reynolds stresses nondimensionalized by the trace of the Reynolds stress tensor. Note that after a moderate amount of total shear, the Reynolds stresses are remarkably close to the values obtained in shear flow experiments such as homogeneous shear [34] and boundary layers [35]. The anisotropy of the initial condition is therefore quite close to that of turbulence in shear flows before it interacts with the shock wave.

Upon compression, the turbulent kinetic energy is amplified; the amplification ratio depends upon the extent of initial shear and is shown in Fig. 2. The kinetic energy is normalized with its initial value (value before compression) and the different curves correspond to different values of initial total shear. As β_o is increased, q^2/q_o^2 increases, indicating that the amplification of ki-

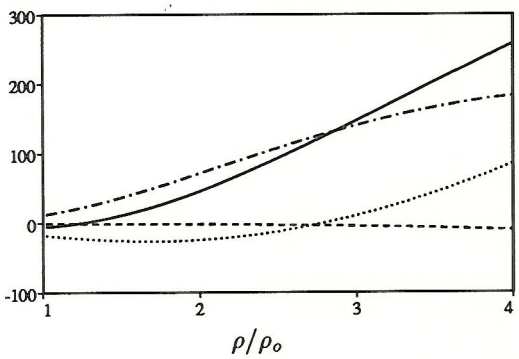

FIGURE 6. Budget of terms in the R_{12} equation ($\beta_o = 3$): —— (LHS), ····· (Strain production), ---- (Shear production), —·— (Pressure strain term)

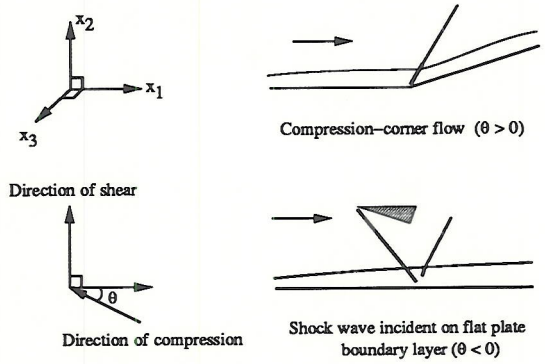

FIGURE 7. Coordinate system used in the analysis of oblique compression of sheared turbulence

netic energy across a normal shock is higher for shear flows than it is for isotropic turbulence. The evolution of the components of turbulent kinetic energy is shown in Fig. 3. The initial total shear is set to 3. All three components are seen to amplify, with the shock-normal velocity component being amplified the most.

Fig. 4 shows the evolution of the diagonal terms of the Reynolds stress anisotropy tensor b_{ij} defined as $b_{ij} = R_{ij}/q^2 - \delta_{ij}/3$. We note the effect of compression to increase the contribution of u_1 to the total kinetic energy, while decreasing that of u_2 and u_3. The figure also shows that the interaction of a shear flow with a normal shock retains the ordering of the components of turbulent kinetic energy ($u_1 > u_3 > u_2$).

We see that the response of sheared turbulence to compression is quite different from that of isotropic turbulence. We attempt to explain this difference in terms of the initial anisotropy as follows. The kinetic energy equation (for $S_o/\Gamma_o \ll 1$) is given by

$$\frac{1}{2}\frac{dq^2}{dt} = -\frac{\Gamma_o}{1+\Gamma_o(t-t_o)}\overline{u_1^2} \qquad (12)$$

For notational convenience, we define $f = \overline{u_1^2}/q^2$ (Note that $f = b_{11} + 1/3$) and rewrite the above equation as

$$\frac{1}{2q^2}\frac{dq^2}{dt} = -\frac{\Gamma_o}{1+\Gamma_o(t-t_o)}f \qquad (13)$$

Denoting f at $t = 0$ by f_o, we note that increasing f_o has the effect of increasing the initial rate of change of kinetic energy and hence the initial kinetic energy amplification. Since, as seen in Fig. 4, compression tends to increase f, this effect of f_o is sustained throughout the evolution; *i.e.*, kinetic energy amplification increases with increasing f_o. This explains the trend seen in Fig. 2. Increasing β_o has the effect of increasing f_o and hence, the kinetic energy amplification.

The evolution of R_{12}/q^2 ($R_{12} = \overline{u_1 u_2}$) upon compression is shown in Fig. 5. where, the three curves correspond to different amounts of initial shear. R_{12}/q^2 decreases in magnitude upon normal compression and, for large compressions it changes sign. This behavior was first observed by Cambon[35] in a different formulation of the normal compression problem, and is hastened upon increasing the initial shear. The cause of this trend was investigated by examining the budget of terms in the R_{12} evolution equation as follows.

The evolution equation for R_{12} is given by

$$\frac{d}{dt}\overline{u_1 u_2} = -\frac{\Gamma_o}{1+\Gamma_o t}\overline{u_1 u_2} - \frac{S_o}{1+\Gamma_o t}\overline{u_2^2} + \pi_{12} \qquad (14)$$

where π_{ij} is the pressure-strain correlation defined as $\pi_{ij} = \overline{p(u_{i,j} + u_{j,i})/\rho}$

Note that both strain production and shear production tend to increase the magnitude of R_{12} (make it more negative). The tendency of $|R_{12}|$ to decrease must therefore be due to the pressure strain correlation. Fig. 6 illustrates the evolution of the R_{12} budget for the case with $\beta_o = 3$. We see that the tendency of R_{12} to change sign is due to amplification of the pressure-strain correlation upon compression.

3.2 Oblique compression

Thus far, we have considered the normal compression of sheared turbulence. However, since shear flows are anisotropic, one would expect the directionality of the compression to be a parameter; *i.e.*, the oblique compression of a shear flow would yield different results from normal compression. The obliquity of compression may be characterized by the angle θ between

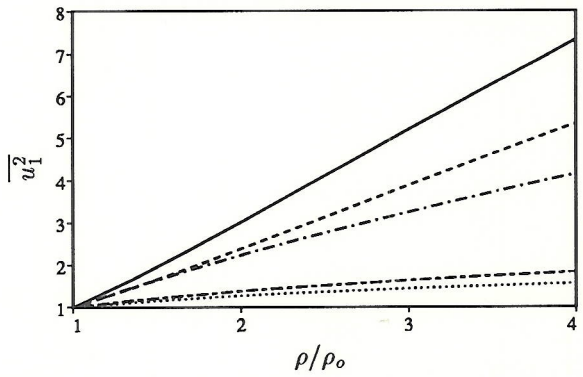

FIGURE 8. Evolution of $\overline{u_1^2}$ for varying oblique angles ($\beta_o = 3$): —— ($\theta = 0°$), ····· ($\theta = -60°$), ---- ($\theta = -30°$), —·— ($\theta = 30°$), —·— ($\theta = 60°$)

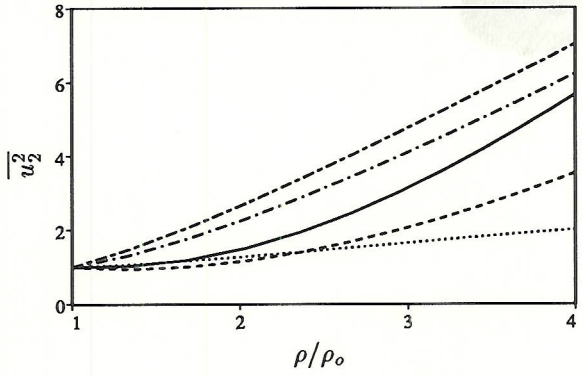

FIGURE 9. Evolution of $\overline{u_2^2}$ for varying oblique angles ($\beta_o = 3$): —— ($\theta = 0°$), ····· ($\theta = -60°$), ---- ($\theta = -30°$), —·— ($\theta = 30°$), —·— ($\theta = 60°$)

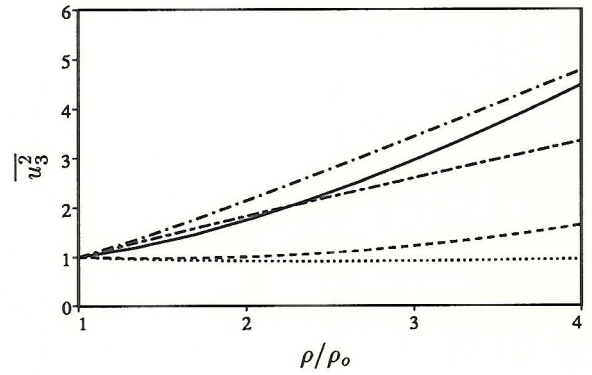

FIGURE 10. Evolution of $\overline{u_3^2}$ for varying oblique angles ($\beta_o = 3$): —— ($\theta = 0°$), ····· ($\theta = -60°$), ---- ($\theta = -30°$), —·— ($\theta = 30°$), —·— ($\theta = 60°$)

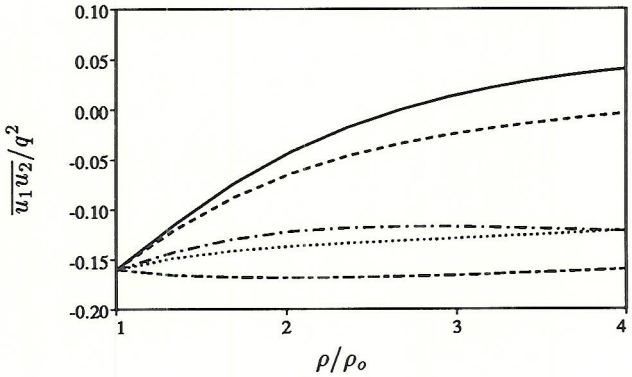

FIGURE 11. Evolution of $\overline{u_1 u_2}/q^2$ for varying oblique angles ($\beta_o = 3$): —— ($\theta = 0°$), ····· ($\theta = -60°$), ---- ($\theta = -30°$), —·— ($\theta = 30°$), —·— ($\theta = 60°$)

the direction of compression and the direction of the upstream shear flow. $\theta = 0$ corresponds to the normal compression discussed so far. RDT using the time-dependent wave number method of solution discussed in Section 2, was used to study the effect of oblique compression. Fig. 7 shows the coordinate system used along with physical situations corresponding to positive and negative angles of obliquity. Note that the shear is assumed to be in the x_2 direction.

The effect of oblique compression on the components of turbulent intensity is shown in Figs. 8,9 and 10. The different curves correspond to different oblique angles of compression. All components are nondimensionalized by their initial values which correspond to sheared turbulence with $\beta_o = 3$. It is clear that obliquity of the compression has a significant effect on kinetic energy evolution. Amplification of $\overline{u_1^2}$ is seen to decrease with increasing oblique angle for both positive and negative angles. The amplification of $\overline{u_2^2}$ and $\overline{u_3^2}$ on the other hand depend on whether the oblique angle is positive or not. In general, the amplification increases with oblique angle for positive angles and decreases for negative angles. This suggests the possibility that oblique compression could change the ordering of turbulent intensity (and hence the nature of the anisotropy) in shear flows.

Fig. 11 shows the evolution of the nondimensional Reynolds shear stress for different oblique angles. Recall that for a normal compression, R_{12}/q^2 decreases and even changes sign. This tendency decreases as the oblique angle increases and for large oblique angles, R_{12}/q^2 amplifies.

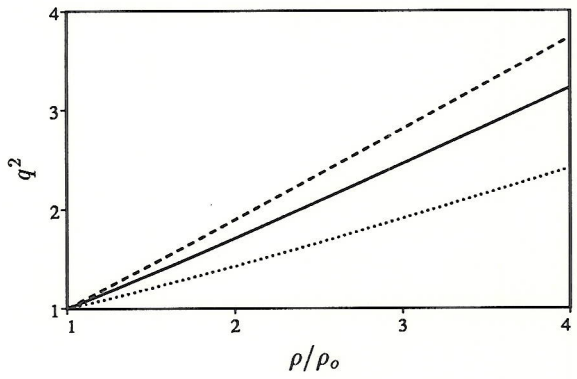

FIGURE 12. Effect of initial anisotropy on q^2 amplification. Initially:: —— (Isotropic), ····· (Contracted), ---- (Expanded),

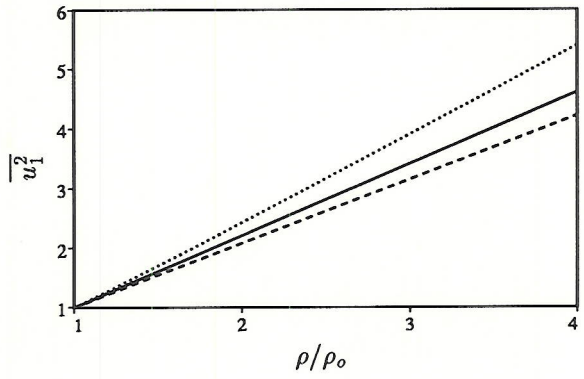

FIGURE 13. Effect of initial anisotropy on $\overline{u_1^2}$ amplification. Initially: —— (Isotropic), ····· (Contracted), ---- (Expanded)

3.3 Comparison to experiment

In this section, we compare the results obtained from RDT to an experiment performed by Smits and Muck [8] on shock wave/boundary layer interaction in a compression-corner. Smits and Muck made measurements of the longitudinal mass flux, $\overline{(\rho u_1)}$ and density weighted Reynolds shear stress, $\overline{(\rho u_1)u_2}$ in three compression-corner flows with corner angles of 8°, 16° and 20° respectively. The free-stream Mach number upstream of the corner was 2.9 in all three cases and, the coordinate system for measurement was aligned with the local direction of the wall. From the measurements made, Morkovin's hypothesis was used to deduce longitudinal velocity fluctuations, (u_1) and the Reynolds shear stress, $\overline{u_1 u_2}$. The flows in the 16° and 20° cases were separated and hence, we restrict our comparison to the 8° case. We compare the evolution of $\overline{u_1 u_2}/\overline{u_1^2}$ and the amplification of $\overline{u_1^2}$ across the shock at y/δ of 0.6 (which is sufficiently away from the wall for wall-blocking effects to be negligible). Experimental data for a more detailed comparison is not available.

To generate an initial state that is close to the experiment, we take β_o as 3.5 for which, $\overline{u_1 u_2}/\overline{u_1^2}$ is 0.25 (same as its experimental value). Recall that the parameters determining the evolution of this initial state are the total volumetric strain (ρ/ρ_o) and the angle between the shear and compression. Both these parameters are obtained by assuming that the upstream flow with a Mach number of 2.9 is turned by 8° across a single shock. Solution of the corresponding inviscid problem yields a shock normal Mach number of 1.29 and an angle of $\theta = 63.65°$ between the shear and strain. The shock normal Mach number is used to determine the density ratio across the shock which is taken as the total volumetric strain. Before we compare the RDT evolution to experiment, we note that in the previous section, our coordinate system was always aligned with the shear which in the experiments, would correspond to the wall upstream of the corner. However downstream of the corner, the experimental coordinate system is no longer aligned with the upstream but changes to align with the local direction of the wall. This amounts to rotation of the Reynolds stress tensor obtained in the analysis in the previous section, by an angle α equal to the angle of the compression corner.

For the volumetric strain and oblique angle indicated above, the analysis yields, $\overline{u_1 u_2}/\overline{u_1^2} = 0.44$ which is remarkably close to the experimental value of 0.45. The amplification of $\overline{u_1^2}$ however, is predicted as 1.06 which is much lower than the experimental value of about 1.4. The amplification of $\overline{u_2^2}$ and $\overline{u_3^2}$ as predicted by RDT are 2.55 and 1.40 respectively. RDT predicts that $\overline{u_1^2}/q^2, \overline{u_2^2}/q^2$ and $\overline{u_3^2}/q^2$ change to 0.48, 0.16 and 0.36 respectively from their initial values of 0.59,0.08 and 0.33. The oblique compression decreases the contribution of $\overline{u_1^2}$ while increasing that of $\overline{u_2^2}$ to the total energy. The ratio $\overline{u_1^2}/\overline{u_2^2}$ is predicted to drop from an initial value of 7.1 to 2.91 after compression.

4. One-dimensional compression of axisymmetric turbulence

In this section, we consider the one-dimensional compression of axisymmetric turbulence. The objective of this study is two-fold: to study how grid turbulence that is passed through a wind-tunnel contraction responds to a normal shock and, to verify our conclusions from the shear flow problem regarding the effect of anisotropy on kinetic energy amplification.

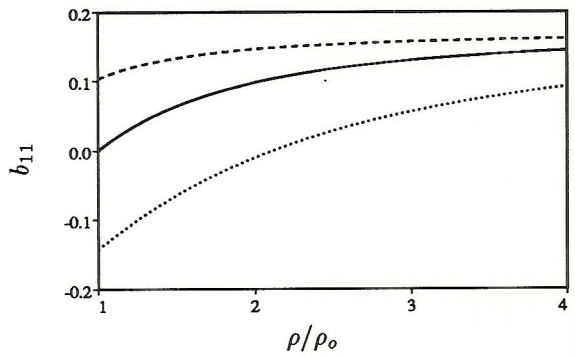

FIGURE 14. Evolution of b_{11} upon one-dimensional compression. Initially: —— (Isotropic), ····· (Contracted), ---- (Expanded)

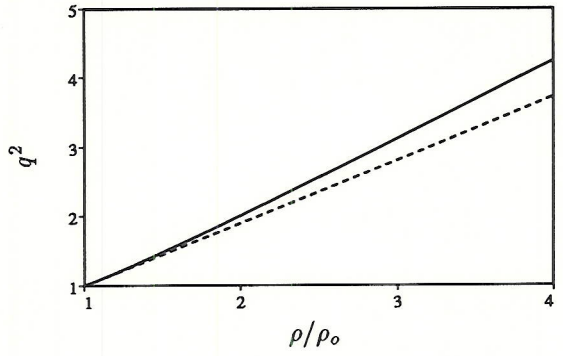

FIGURE 15. Comparison of the amplification of q^2 between sheared and axisymmetric turbulence (Initial $\overline{u_1^2}/q^2 = 0.44$ for both): —— (Sheared), ····· (Axisymmetric)

To generate axisymmetric turbulence, isotropic turbulence is subjected to homogeneous axisymmetric strain; *i.e.*,

$$U_1 = \alpha x_1, \quad U_2 = -\frac{\alpha}{2}x_2, \quad U_3 = -\frac{\alpha}{2}x_3, \quad \rho = \rho_o \quad (15)$$

where U_1, U_2 and U_3 are the mean velocity components in the x_1, x_2 and x_3 directions respectively, and ρ is the mean density, which is uniform. $\alpha > 0$ corresponds to axisymmetric contraction, while $\alpha < 0$ corresponds to axisymmetric expansion. The above strain is applied till a non-dimensional time, αt_o when it is replaced by the one-dimensional compression given by equations (5) through (7). Axisymmetrically strained turbulence is thus, the initial condition for the one-dimensional compression. Regarding the nature of the anisotropy in the initial state, note that under RDT, axisymmetric contraction suppresses fluctuations along the axis of axisymmetry (x_1) and asymptotes to $\overline{u_1^2}/q^2 = 0$, while axisymmetric expansion enhances fluctuations along x_1 and asymptotes to $\overline{u_1^2}/q^2 = 1/2$. (for details, see 28).

In the previous section, we observed that the amplification of q^2 in the normal compression of sheared turbulence was higher than that for isotropic turbulence; an effect that was attributed to initial $\overline{u_1^2}/q^2$ being higher in the sheared turbulence. We check this effect of the initial anisotropy in Fig. 12 where the evolution of q^2 is plotted against the total volumetric strain. The three curves correspond to initially isotropic turbulence, initially contracted turbulence ($\alpha t_o = 0.5$ yielding an initial $\overline{u_1^2}/q^2$ of 0.19) and initially expanded turbulence ($\alpha t_o = -0.5$ yielding an initial $\overline{u_1^2}/q^2$ of 0.44) respectively. Since contraction decreases $\overline{u_1^2}/q^2$ and expansion increases it, the amplification of q^2 for contracted turbulence is lower than that for isotropic turbulence whose amplification in turn, is lower than that for expanded turbulence.

Since the axis of initial axisymmetry coincides with the direction of compression, the axisymmetry is retained. Fig. 13 shows the effect of initial anisotropy on the evolution of $\overline{u_1^2}$. We note that the compression tends to amplify $\overline{u_1^2}$; however unlike q^2, the amplification of $\overline{u_1^2}$ *decreases* with increasing initial $\overline{u_1^2}/q^2$.

Axisymmetry ($\overline{u_2^2} = \overline{u_3^2}$) enables us to compute $\overline{u_2^2}$ and $\overline{u_3^2}$ from q^2 and $\overline{u_1^2}$. From Figs. 12 and 13, we see that these velocity components are amplified and that their amplification ratio increases with increasing initial $\overline{u_1^2}/q^2$. The change in the anisotropy of Reynolds stress is of interest and is plotted in Figure 14. Due to axisymmetry, $b_{22} = b_{33} = -b_{11}/2$ and hence, only b_{11} is shown. The three curves correspond to initially isotropic, contracted and expanded turbulence respectively. Note that all three curves show an increase in b_{11}, indicating that irrespective of initial anisotropy, the effect of the one dimensional compression is to increase the contribution of u_1 to the total energy (and decrease that of u_2 and u_3). Though not shown in Fig. 14, we mention that in the limit of infinite volumetric strain, b_{11} becomes independent of initial anisotropy and becomes equal to 1/6 (its asymptotic value for initially isotropic turbulence).

Thus far, we have seen the importance of initial anisotropy defined in terms of $\overline{u_1^2}/q^2$ on the amplification of kinetic energy. It is of interest to see if $\overline{u_1^2}/q^2$ is the only significant parameter of the initial field. We do so by comparing the effect of normal compression upon

sheared turbulence with that on axisymmetrically expanded turbulence. The amount of total shear (β_o) and total axisymmetric strain (αt_o) are chosen such that both initial states have the same $\overline{u_1^2}/q^2$ of 0.44.

Fig. 15 compares the amplification of q^2 between the two flows. The two curves are different, indicating that $\overline{u_1^2}/q^2$ is not the sole parameter. However, the extent of disagreement between the two curves is not very large for moderate total strains. For example, at a density ratio of 3, which corresponds to a normal Mach number of about 2.25, q^2 in the shear flow is amplified by 3.15 while the amplification ratio of q^2 in the axisymmetric flow is 2.8; a difference of 10%. A qualitative difference noticed between the two flows concerns the amplification of $\overline{u_1^2}$. For axisymmetric turbulence, the amplification of $\overline{u_1^2}$ was seen to decrease with increasing initial $\overline{u_1^2}/q^2$. However this trend is reversed for sheared turbulence (figure not shown) where the amplification of $\overline{u_1^2}$ was seen to increase with initial $\overline{u_1^2}/q^2$.

5. Conclusion

Inviscid, incompressible rapid distortion theory was used to study the response of anisotropic turbulence to a shock wave. Two problems were studied; one-dimensional compression of sheared turbulence and compression of axisymmetric turbulence along the axis of axisymmetry.

In the sheared turbulence problem, both normal and oblique compressions were studied. Normal compression is seen to amplify all components of turbulent kinetic energy with the component normal to the shock being amplified the most. For a given total volumetric strain, the total kinetic energy amplification ratio increases as the amount of initial shear increases. This effect of initial anisotropy on kinetic energy amplification is attributed to the initial value of $\overline{u_1^2}/q^2$ (x_1 is the shock-normal direction). The total kinetic energy amplification increases with increasing initial $\overline{u_1^2}/q^2$. Normal compression tends to decrease the magnitude of the non-dimensional Reynolds shear stress (R_{12}/q^2) and for large volumetric strains even changes its sign. Increasing the initial total shear is seen to hasten this behavior. Examination of the budget of terms in the R_{12} equation shows this behavior is due to the pressure-strain correlation.

The obliquity of compression, characterized by the angle between the initial shear and the compression is seen to affect the turbulence evolution considerably. The amplification of the streamwise (with respect to the shear) velocity fluctuations is seen to decrease with increasing oblique angle, while the amplification of the transverse components increases for positive oblique angles and decreases for negative angles. Obliquity is seen to reduce the tendency of the magnitude of R_{12} to decrease upon compression and for large oblique angles R_{12} amplifies. Comparison of RDT to a compression-corner experiment by Smits and Muck shows good agreement in $\overline{u_1 u_2}/\overline{u_1^2}$ while the amplification of $\overline{u_1^2}$ is below the experimental value.

The effect of initial $\overline{u_1^2}/q^2$ on the amplification of q^2 is verified in the one-dimensional compression of axisymmetric turbulence where the amplification of q^2 for initially expanded turbulence is higher than that for isotropic turbulence which in turn is higher than that of contracted turbulence. Once again compression is seen to amplify all components of turbulence intensity. The amplification of u_1^2 however, decreases with increasing initial $\overline{u_1^2}/q^2$ unlike the amplification of $\overline{u_2^2}$ and q^2 which increase.

Acknowledgement

We gratefully acknowledge the financial support provided by AFOSR under Grant No. 88-NA-322 with Dr. Leonard Sakell as the technical monitor. Computing resources made available by NASA Ames Research Center and the NAS facility are greatly appreciated. We are also thankful to Dr. S. Lee for many useful discussions.

References

1. Viegas, J.R. and Horstman, C.C., 1979, Comparison of Multi-equation Turbulence Models for Several Shock Boundary-Layer Interaction Flows, *AIAA Journal*, Vol. 17, No. 6, pp. 811-820.
2. Settles, G.S., Fitzpatrick, T.J., Bogdonoff, S.M., 1979, Detailed Study of Attached and Separated Compression Corner Flowfields in High Reynolds Number Supersonic Flow, *AIAA Journal*, Vol. 17, No. 6, pp. 579-585.
3. Debieve, F.R., Gouin, H., Gaviglio, J., 1982, Evolution of the Reynolds Stress Tensor in a Shock Wave - Turbulence Interaction, *Indian Journal of Technology*, Vol. 20, pp. 90-97.
4. Dolling, D.S., Orr, C.T., 1985, Unsteadiness of the Shock Wave Structure in Attached and Separated Compression Ramp Flows, *Experiments in Fluids*, **3**, pp. 24-32.
5. Andreopoulos, J., Muck, K.C., 1987, Some New Aspects of the Shock Wave Boundary Layer Interaction in Compression ramp Corner, *J. Fluid Mech.*, **180**, pp. 405-428.

6. Dussauge, J.P., Muck, K.C., Andreopoulos, J., 1986, Properties of wall Pressure Fluctuations in a Separated Flow over a Compression Ramp , *Turbulent Shear Layer/Shock Wave Interactions* , edited by J. Delery , Springer, Berlin.
7. Jayaram, M., Taylor, M.W., Smits, A.J., 1987, The Response of a Compressible Turbulent Boundary Layer to Short Regions of Concave Surface Curvature, *J. Fluid Mech.*, **175**, pp. 343-362.
8. Smits, A.J., Muck, K.C., 1987, Experimental Study of Three Shock Wave/ Turbulent Boundary Layer Interactions, *J. Fluid Mech.*, **182**, pp. 294-314.
9. Kuntz, D.W., Amatucci, V.A., Addy, A.L., 1987, Turbulent Boundary Layer Properties Downstream of the Shock Wave/ Boundary Layer Interaction, *AIAA Journal*, Vol. 25, No. 5, pp. 668-675.
10. Selig, M.S., Andreopoulos, J., Muck, K.C., Dussauge, J.P., Smits, A.J., 1989, Turbulent Structure in a Shock Wave/ Turbulent Boundary Layer Interaction, *AIAA Journal*, Vol. 27, No. 7, pp. 862-869.
11. Debieve, J.F., Lacharme, J.P, 1986, A Shock Wave /Free Turbulence Interaction, In *Turbulent Shear Layer/Shock Wave Interactions* edited by J. Delery, Springer, Berlin
12. Jacquin, L., Blin, E., Geffroy, P., 1991, Experiments on Free Turbulence /Shock wave Interaction , *Eighth Symposium on Turbulent Shear Flows*, Munich, September 9-11, 1991.
13. Keller, J., Merzkirch, W., 1990, Interaction of a Normal Shock Wave with a Compressible Turbulent Flow, *Experiments in Fluids*, **8**, pp. 241-248.
14. Honkan, A., Andreopoulos, J., 1990, Experiments in a Shock Wave/ Homogenous Turbulence Interaction, *AIAA Paper*, No. 90-1647.
15. Lee, S, Lele, S.K., Moin, P, 1991a, Direct Numerical Simulation and Analysis of Shock Turbulence Interaction, *AIAA Paper*, No. 91-0523.
16. Rotman, D, 1991, Shock wave Effects on a Turbulent Flow, *Phys. Fluids A*,**3**, pp. 1792-1806.
17. Lee, S, Lele, S.K., Moin, P, 1992, Interaction of Isotropic Turbulence with a Shock Wave, *Report No. TF-52*, Thermosciences Division, Dept. of Mech. Engg., Stanford University.
18. Ribner, H.S., 1954, Shock-Turbulence Interaction and the Generation of Noise, *NACA TN 3255*
19. Moore, F.K., 1954, Unsteady Oblique Interaction of a Shock Wave with a Plane Disturbance, *NACA TN 2879*
20. Chang, C.T., 1957, Interaction of a Plane Shock and Oblique Plane Disturbances with Special Reference to Entropy Waves, *J. Aero. Sci.*, Vol. 24, pp. 675-682.
21. Kerrebrock, J.L., 1956, The Interaction of Flow Discontinuities with Small Disturbances in a Compressible Fluid, *Ph.D Thesis, CalTech*
22. McKenzie, J.F., Westphal, K.O., 1968, Interaction of Linear Waves with Oblique Shock Waves, *Phys. Fluids*, Vol. 11, pp. 2350-2362.
23. Sekundov, A.N., 1974, Supersonic Flow Turbulence and Interaction with a Shock Wave, *Akademia Nauk, USSR, Izvestia Mekhanika Zhidkosti i Gaza*, March-April 1974.
24. Dosanjh, D.S., Weekes, T.M., 1964, Interaction of a Starting Vortex as well as Karman Vortex Streets with Travelling Shock Wave, *AIAA Paper No. 64-425*
25. Zang, T.A., Hussaini, M.Y., Bushnell, D.M., 1984, Numerical Computations of Turbulence Amplification in Shock-Wave Interactions, *AIAA Journal*, Vol. 22, pp. 13-21.
26. Rogallo, R.S., 1981, Numerical Experiments in Homogeneous Turbulence, *NASA Tech. Memo. 81315*
27. Cambon, C., Coleman, G.N. and Mansour, N.N., 1992, Rapid distortion analysis and direct simulation of compressible homogeneous turbulence at finite Mach number, *Proceedings of the Summer Program 1992, Center for Turbulence Research.*
28. Batchelor, G.K. and Proudman, I., 1954, The Effect of Rapid Distortion on a Fluid in Turbulent Motion, *Quart. J. Mech. Appl. Math.* **7**, 83-103.
29. Lee, M.J., 1989, Distortion of homogeneous turbulence by axisymmetric strain and dilatation, *Phys. Fluids A* **1**, 1541-1557.
30. Moffatt, H.K., 1967, *Proceedings of the International Colloquium on Atmospheric Turbulence and Radio Wave Propagation*, Moscow, June 1965, pp. 139-156.
31. Townsend, A.A., 1970, *J. Fluid Mech.*, Vol. 41, pp. 13-46.
32. Lee, M.J., Kim, J., Moin, P., Structure of high turbulence at high shear rate, *J. Fluid Mech.*, Vol. 216, pp. 561-583.
33. Rogers, M.M., 1991, The structure of a passive scalar field with a uniform mean gradient in rapidly sheared homogeneous turbulent flow, *Phys. Fluids A*, **3**, pp. 144-154.
34. Tavoularis, S., Karnik, U., 1989, Further experiments on the evolution of turbulent stresses and scales in uniformly sheared turbulence, *J. Fluid Mech.*, Vol. 204, pp. 457-478.
35. Townsend. A.A., 1976 Structure of Turbulent Shear Flow, Cambridge University Press
36. Cambon, C., 1990, Private communication.